

A Model for Zebrafish Ventricular Action Potential

Ludovica Cestariolo¹, Marina Battaller Martinez², Jose M Ferrero², Jose F Rodriguez Matas¹

¹Politecnico di Milano, Milan, Italy

²Universitat Politècnica de Valencia, Valencia, Spain

Abstract

From the '90s, the interest in the use of zebrafish has exponentially grown thanks to the numerous characteristics, very close to the human ones, that make this little fish very attractive in different fields. Thus, zebrafish has been increasingly proposed as a pharmacological and genetic screening model. The growing interest and the relevance of this animal model motivate the development of a mathematical model of the action potential of the zebrafish to facilitate the understanding of the mechanisms associated with its electrophysiological behavior and how they correlated with those observed in humans.

This work presents the first attempt to develop a mathematical model of the adult zebrafish action potential. The model is based on the Ten Tusscher formulation of the action potential of human cardiomyocyte in which the main currents have been reparametrized to be adapted to those of the zebrafish, while extending the model to account for the T-type calcium current present in the zebrafish. Preliminary results of the proposed model show an action potential morphology in good agreement with experimental data.

1. Introduction

The numerous similarities between the physiology of the zebrafish and the human have attracted the attention of researchers from different fields toward this little fish. Of particular interest is the resemblance in the action potential due to the presence of ~ 69% of human genes orthologues [1] that lead to a functional similarity in cardiac ion channels [2] and the shape and duration of the action potential (AP). Thus, zebrafish has been increasingly proposed as a pharmacological and genetic screening model for studies of cardiotoxicity.

Given the growing interest and the relevance of this animal model, developing an action potential model for the zebrafish is important to study pathologies and drug administration in-silico, in addition to better understand the ionic mechanisms involved in the development of a given pathology or the response to a particular drug. For

this reason, this work aims at developing a mathematical model of the action potential based on literature data on ionic channels.

2. Methods

This work develops an electrophysiological detailed action potential model of the zebrafish from the Ten Tusscher and Panilov (TP06) formulation for human cardiomyocytes [3][4]. The approach consists in reparametrizing the main currents to adapt them to the zebrafish, while introducing new current based on formulations used in other models of the action potential and parametrized to the zebrafish. The choice of the TP06 model as the base model was made because of the similarities between zebrafish and humans and its highly computationally cost-effectiveness.

2.1. Ionic channels

To develop a detailed AP model, experimental data were necessary. For this reason, an extensive literature review was performed to account for the most recent experimental data regarding the main currents present in the zebrafish (i.e., patch-clamp data). In addition to individual channel data, electrophysiological information associated with the whole cell response (i.e., AP waveform and calcium transient, at different heart rates, necessary for further model validation) was collected.

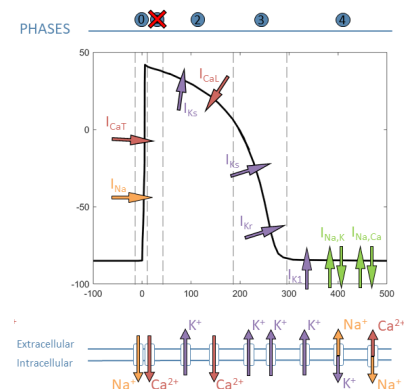


Figure 1. Main phases and currents in the zebrafish AP. Experimental data from [5].

From the analysis, it emerged that the principal currents present in the zebrafish, reported in Figure 1 are: i) the fast sodium current I_{Na} , responsible for the rapid depolarization that occurs during *Phase 0* of the AP and which shows a smaller density with respect to humans [6]; ii) the T-type calcium current I_{CaT} , that contributes to the initial upstroke in *Phase 0* [7], and iii) the L-type calcium current I_{CaL} that maintain the long plateau phase (*Phase 2*) and provide activator of Ca^{2+} for contraction [8]. iv) The slow delayed rectifier current I_{Ks} and v) the rapid delayed rectifier current I_{Kr} , respectively responsible in *Phase 2* with less density [9] and *Phase 2/3* with higher density in zebrafish than in humans [10], and vi) the inward rectifier potassium current I_{K1} , that contributes returning to the resting potential during *Phase 4* and shows a smaller density with respect to humans [11]. Finally, vii) Na^+/K^+ pump, and viii) Na^+/Ca^{2+} exchanger, both responsible during *Phase 4* of the AP.

It is therefore evident that the main differences between zebrafish and humans lie in the absence of the transient outward current I_{to} , and consequently in the lack of the peak and dome feature in the AP[12], and in the crucial role that I_{CaT} assumes in the zebrafish in opposition to its marginal role in humans. In fact, the presence of I_{CaT} in the adult mammalian heart is mainly limited to the sinoatrial node and conductive pathways [12].

2.2. Action potential model

As described in the previous paragraph, the main differences between the zebrafish and human AP are related to the lack of the transient outward current I_{to} which was removed from the model, and the importance of the I_{CaT} that is missed in the TT model. The mathematical model of the zebrafish action potential is then represented as:

$$C_m \frac{dV}{dt} = -I_{ion} - I_{stim} \quad (1)$$

where V is the transmembrane voltage, t is time, I_{stim} is the externally applied stimulation current, C_m is the cell membrane capacitance per unit surface area, and I_{ion} is the sum of the ionic currents given by the following equation:

$$I_{ion} = I_{Na} + I_{CaL} + I_{CaT} + I_{K1} + I_{Kr} + I_{Ks} + I_{NaCa} + I_{NaK} + I_{pCa} + I_{pK} + I_{bCa} + I_{bNa} \quad (2)$$

For most of the currents, the same formulation proposed in the TP06 model was assumed, reparametrizing the steady-state and time constant curves of the different gating variables, to fit experimental data reported for the zebrafish. Figure 2 shows, as an example, the reparametrized curves for the fast sodium current I_{Na} .

In other cases, the formulation has been slightly modified to better fit experimental data, as is the case of the inward rectifying current, I_{K1} , defined in the TP06 model as

$$I_{K1} = g_{K1} \sqrt{\frac{[K^+]_o}{5.4}} \chi_{K1\infty} (V - E_K), \quad (3)$$

where g_{K1} the maximum channel conductance, $[K^+]_o$ the extracellular potassium concentration, E_K is the reversal potential of potassium, and $\chi_{K1\infty}$ a time independent inward rectifying factor that is function of the potential defined for the zebrafish as

$$\chi_{K1\infty} = \frac{1}{1 + e^{\frac{V+81.5}{13.24}}} \quad (4)$$

to best fit the experimental data from [11].

The rapid and slow rectifying currents, I_{Kr} and I_{Ks} respectively, were also slightly modified with respect to the original TP06 formulation. The formulation of the I_{Kr} was reformulated by introducing a fast and slow activation gate to accommodate the experimental data from [10], leading to

$$I_{Kr} = g_{Kr} \sqrt{\frac{K_o}{5.4}} x_{r1f} x_{r1s} x_{r2} (V - E_K), \quad (5)$$

where g_{Kr} is the maximum conductance of the channel, x_{r1f} and x_{r1s} are the fast and slow activation gates respectively, and x_{r2} the inactivation gate.

For the case of I_{Ks} , on the contrary, the original TP06 formulation was modified by considering only one inactivation gate since it was found to better fit the experimental data from [9]

$$I_{Ks} = g_{Ks} x_s (V - E_{Ks}), \quad (6)$$

where g_{Ks} is the maximum conductance of the channel, x_s is an activation gate and E_{Ks} is a reversal potential determined by a large permeability to potassium and a small permeability to sodium ions as defined in [3]. For both currents I_{Ks} and I_{Kr} the formulation from TP06 for the gating variables has been assumed reparametrized to fit experimental data for the zebrafish.

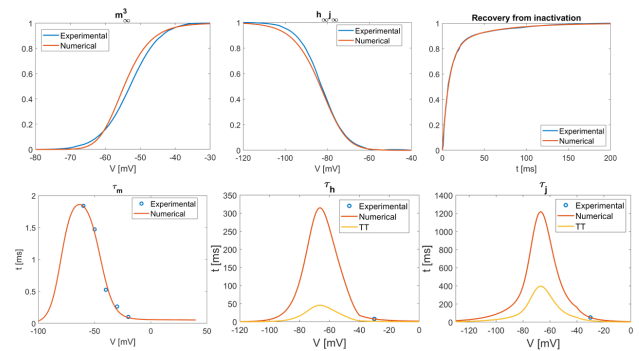


Figure 2. Steady-state and time constant curves describing the gating of the fast Na^+ current. Experimental data are from Chopra et al., 2007 [6]. A: Steady-state activation. B: Steady-state inactivation. C: Activation time constants. E: Fast inactivation time constants. F: Slow inactivation time constants. τ_h and τ_j were obtained by scaling the original TP06 curves [3] due to the difference in body temperature between human and zebrafish (37 °C and 23 °C).

Regarding the sarcolemma calcium currents, I_{CaL} and I_{CaT} , the formulation for I_{CaL} from the TP04 model was adopted, reparametrizing the voltage dependent activation and slow inactivation gates according to the data from [13]. The calcium dependent inactivation gate was left invariant. For the T-type calcium current, I_{CaT} , the formulation proposed in [14][15] for the rabbit sino-atrial node was adopted and the gating variables reparametrized to fit current-potential curves of the zebrafish reported in [7].

With respect to the sodium calcium exchanger, I_{NaCa} , and the sodium potassium pump, I_{NaK} , the same formulation present in the TP06 model was adopted since no experimental data for the zebrafish is available to date. Further, the intracellular calcium formulation from the original TP06 model with small modifications to incorporate the T-type calcium current has been adopted in this version of the model.

After formulating the behavior for the different gating variables, a Monte Carlo simulation that varied all ionic conductances simultaneously was conducted to select the combination that best fit the shape of the action potential to experiments while rendering the model stable. The Monte Carlo simulation consisted in stimulating the model with a trend of 110 stimulus at a frequency of 1 Hz followed by 3 seconds without stimulation. The last 10 action potentials and the last 3 seconds of the simulation were saved for analysis. A given combination of parameters (ionic conductances) was considered valid if the results showed absence of alternants in the last ten APs and pacemaking behavior after interrupting the stimulation. The model has been implemented in matlab R2021a (Mathworks Inc.), the gates have been integrated using the Rush-Larsen scheme, and a fixed time step of 0.02 ms has been used for the simulations.

3. Results

The model resulted in a stable AP with all the characteristic of the zebrafish AP as shown in Figure 3 namely, a fast repolarization phase, the absence of the peak and dome and the presence of a well-defined plateau.

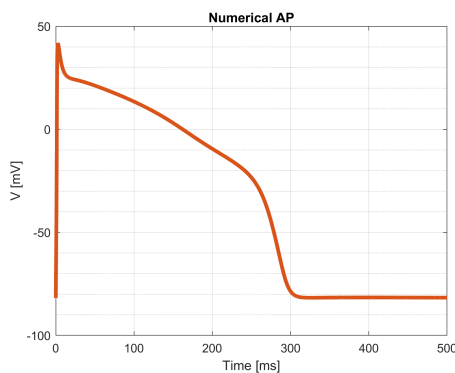


Figure 3. Modeled action potential of the zebrafish.

A more quantitative analysis of the different features characterizing the modeled AP is given in Table 1. The results show all features to be within the range of experimental values.

Table 1. Comparison of AP characteristics between model and experiments [5].

AP marker	Model	Experiment
RMP (mV)	-81.74	-89.88 ÷ -76.92
APA (mV)	123.61	115.99 ÷ 138.21
APD ₂₀ (ms)	77.6	-
APD ₅₀ (ms)	241.2	181.2 ÷ 270.98
APD ₉₀ (ms)	291	270.98 ÷ 435
dV/dt _{depol} (V/s)	113.52	39.42 ÷ 166.72
dV/dt _{repol} (V/s)	-2.7	-7.2 ÷ -1.39

4. Discussion

This work presents the first attempt to develop an action potential model for the adult zebrafish. The model accounts for the major transmembrane currents that have been characterized for this animal model together with the intracellular ion dynamics. Mainly developed from the reparametrization of a well-established human action potential model, the TP06 model, it emerged that the obtained action potential model well describes the main features of the action potential waveform of the zebrafish.

In analyzing the results and evaluating the behavior of the model, it is important to consider that the variability in the experimental AP is very large, as shown in Figure 4 and in Table 1.

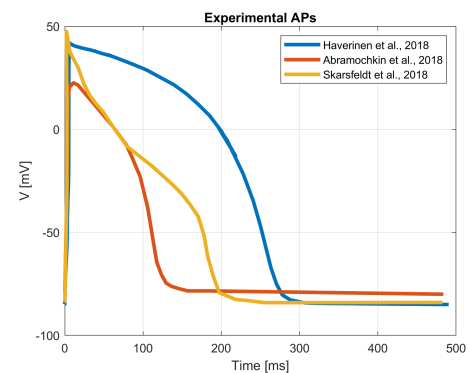


Figure 4. Variability of the action potentials in experimental data [5] [9] [16].

The variability observed in the experimental data may be associated with the rapid development of the zebrafish. Moreover, some studies have reported how the different temperatures in which the experiments are conducted and the used protocol can influence the AP recording [17]. For this reason, in this work, the numerical AP morphology was compared with experiments using the largest number of features possible. In addition, for the comparison reported in Table 1, the work from *Haverinen et al.* [5] on

isolated ventricular myocytes in correspondence with the numerical simulation of the AP model.

All the AP features evaluated and reported in literature [5] were compared with the numerical model. Table 1 shows that all the numerical values describing the features of the AP waveform are within the experimental range. However, these results have to be considered as preliminary and further tests regarding AP adaptability (response to different stimulating frequencies) together with the response to drugs has to be investigated to determine the validity of the proposed model.

5. Conclusion and future developments

This paper presents for the first time an electrophysiologically detailed model of the action potential model of the zebrafish able to reproduce the main features of the AP waveform. However, the model is not exempt from limitations and further improvements and investigations are required. In particular, it will be necessary to study in more detail the calcium dynamics by comparing the transients against experiments. Also, a careful sensitivity analysis of the impact that the formulation of the $\text{Na}^+/\text{Ca}^{2+}$ exchanger and the Na^+/K^+ pump have on the model performance and behavior has to be evaluated in detail.

References

- [1] K. Howe *et al.*, “The zebrafish reference genome sequence and its relationship to the human genome,” *Nature*, vol. 496, no. 7446, p. 498, Apr. 2013, doi: 10.1038/NATURE12111.
- [2] U. Ravens, “Ionic basis of cardiac electrophysiology in zebrafish compared to human hearts,” *Prog. Biophys. Mol. Biol.*, vol. 138, pp. 38–44, Oct. 2018, doi: 10.1016/J.PBIOMOLBIO.2018.06.008.
- [3] K. H. W. J. Ten Tusscher, D. Noble, P. J. Noble, and A. V. Panfilov, “A model for human ventricular tissue,” *Am. J. Physiol. Heart Circ. Physiol.*, vol. 286, no. 4, 2004, doi: 10.1152/AJPHEART.00794.2003.
- [4] K. H. W. J. Ten Tusscher and A. V. Panfilov, “Alternans and spiral breakup in a human ventricular tissue model,” *Am. J. Physiol. Heart Circ. Physiol.*, vol. 291, no. 3, 2006, doi: 10.1152/AJPHEART.00109.2006.
- [5] J. Haverinen, M. Hassinen, H. Korajoki, and M. Vornanen, “Cardiac voltage-gated sodium channel expression and electrophysiological characterization of the sodium current in the zebrafish (*Danio rerio*) ventricle,” *Prog. Biophys. Mol. Biol.*, vol. 138, pp. 59–68, Oct. 2018, doi: 10.1016/J.PBIOMOLBIO.2018.04.002.
- [6] S. S. Chopra, H. Watanabe, T. P. Zhong, and D. M. Roden, “Molecular cloning and analysis of zebrafish voltage-gated sodium channel beta subunit genes: implications for the evolution of electrical signaling in vertebrates,” *BMC Evol. Biol.*, vol. 7, 2007, doi: 10.1186/1471-2148-7-113.
- [7] J. Haverinen, M. Hassinen, S. N. Dash, and M. Vornanen, “Expression of calcium channel transcripts in the zebrafish heart: dominance of T-type channels,” *J. Exp. Biol.*, vol. 221, no. Pt 10, May 2018, doi: 10.1242/JEB.179226.
- [8] P. C. Zhang, A. Llach, X. Y. Sheng, L. Hove-Madsen, and G. F. Tibbits, “Calcium handling in zebrafish ventricular myocytes,” *Am. J. Physiol. Regul. Integr. Comp. Physiol.*, vol. 300, no. 1, Jan. 2011, doi: 10.1152/AJPREGU.00377.2010.
- [9] D. V. Abramochkin, M. Hassinen, and M. Vornanen, “Transcripts of Kv7.1 and MinK channels and slow delayed rectifier K⁺ current (I_{Ks}) are expressed in zebrafish (*Danio rerio*) heart,” *Pflugers Arch.*, vol. 470, no. 12, pp. 1753–1764, Dec. 2018, doi: 10.1007/S00424-018-2193-1.
- [10] E. P. Scholz *et al.*, “Biophysical properties of zebrafish ether-à-go-go related gene potassium channels,” *Biochem. Biophys. Res. Commun.*, vol. 381, no. 2, pp. 159–164, Apr. 2009, doi: 10.1016/J.BBRC.2009.02.042.
- [11] M. Hassinen, J. Haverinen, M. E. Hardy, H. A. Shiels, and M. Vornanen, “Inward rectifier potassium current (I_{K1}) and Kir2 composition of the zebrafish (*Danio rerio*) heart,” *Pflugers Arch.*, vol. 467, no. 12, pp. 2437–2446, Dec. 2015, doi: 10.1007/S00424-015-1710-8.
- [12] M. Vornanen and M. Hassinen, “Zebrafish heart as a model for human cardiac electrophysiology,” *Channels*, vol. 10, no. 2, pp. 101–110, Jan. 2016, doi: 10.1080/19336950.2015.1121335.
- [13] S. N. Kompella, F. Brette, J. C. Hancox, and H. A. Shiels, “Phenanthrene impacts zebrafish cardiomyocyte excitability by inhibiting I_{Kr} and shortening action potential duration,” *J. Gen. Physiol.*, vol. 153, no. 2, Jan. 2021, doi: 10.1085/JGP.202012733.
- [14] S. S. Demir, J. W. Clark, C. R. Murphey, and W. R. Giles, “A mathematical model of a rabbit sinoatrial node cell,” *Am. J. Physiol.*, vol. 266, no. 3 Pt 1, 1994, doi: 10.1152/AJPCELL.1994.266.3.C832.
- [15] H. Zhang *et al.*, “Mathematical models of action potentials in the periphery and center of the rabbit sinoatrial node,” *Am. J. Physiol. Heart Circ. Physiol.*, vol. 279, no. 1, 2000, doi: 10.1152/AJPHEART.2000.279.1.H397.
- [16] M. A. Skarsfeldt, S. H. Bomholtz, P. R. Lundegaard, A. Lopez-Izquierdo, M. Tristani-Firouzi, and B. H. Bentzen, “Atrium-specific ion channels in the zebrafish-A role of I_{KACH} in atrial repolarization,” *Acta Physiol. (Oxf.)*, vol. 223, no. 3, Jul. 2018, doi: 10.1111/APHA.13049.
- [17] E. Lin *et al.*, “Optical mapping of the electrical activity of isolated adult zebrafish hearts: acute effects of temperature,” *Am. J. Physiol. Regul. Integr. Comp. Physiol.*, vol. 306, no. 11, Jun. 2014, doi: 10.1152/AJPREGU.00002.2014.

Address for correspondence:

Ludovica Cestariolo
 LaBS, Dept. of Chemistry, Materials and Chemical Engineering
 “Giulio Natta”, Politecnico di Milano
 Piazza L. Da Vinci, 32, 20133 Milan, Italy
 ludovica.cestariolo@polimi.it